High Voltage

Research Article

IET Journals
The Institution of Engineering and Technology

Effect of long-term fluorination on surface electrical performance of ethylene propylene rubber

eISSN 2397-7264
Received on 17th January 2019
Revised 22nd April 2019
Accepted on 8th May 2019
E-First on 26th June 2019
doi: 10.1049/hve.2019.0005
www.ietdl.org

Rujia Men[1], Zhipeng Lei[1,2], Tao Han[2,3], Davide Fabiani[2], Chuanyang Li[2] ✉, Simone Vincenzo Suraci[2], Jian Wang[4]

[1]*Shanxi Key Laboratory of Mining Electrical Equipment and Intelligent Control, College of Electrical and Power Engineering, Taiyuan University of Technology, Taiyuan 030024, People's Republic of China*

[2]*Department of Electrical, Electronic, and Information Engineering, 'Guglielmo Marconi', University of Bologna, Viale Risorgimento 2, Bologna 40136, Italy*

[3]*Key Laboratory of Smart Grid of Education Ministry, School of Electrical and Information Engineering Tianjin University, Tianjin 300072, People's Republic of China*

[4]*State Key Laboratory of Alternate Electrical Power System with Renewable Energy Sources, North China Electric Power University, Changping District, Beijing 102206, People's Republic of China*

✉ *E-mail: lichuanyangsuper@163.com*

Abstract: To investigate the effect of fluorination on surface electrical performance of ethylene propylene rubber (EPR), four pieces of EPR specimens are prepared and fluorinated for different duration ranging from 120 min to 480 min. The surface morphology and element compositions of experimental specimens are tested. The surface potential decay and complex permittivity are measured. The tracking discharge property and the erosion properties after tracking test are investigated. The surface charge transport and electrical property tailoring mechanism are discussed. The results show that when the fluorination duration is from 120 min to 360 min, the surface morphology gradually becomes flat and compact with time, and the surface resistance to electrical tracking is improved. While an excessive fluorination with the duration of 480 min leads to a significant increase in surface conductivity and a weakening in the resistance to electrical tracking, which is mainly due to a change in surface morphology. The recommended fluorination duration for an optimised surface property is between 240 and 360 min for EPR specimen.

1 Introduction

Due to excellent electrochemical performance and corrosion resistant properties [1, 2], ethylene propylene rubber (EPR) is widely used as dielectric materials of cables operating in coal mine, electric power plant, and submarine [3, 4]. However, during operating, EPR usually suffers from combination stresses, i.e. temperature variation, high electric field, high relative humidity etc. The combined stresses can break C–H and C=C bonds, which lead to aging of dielectrics within a normal service period of time [5]. Fig. 1 shows an EPR insulated cable withdrawn from a coal mine, which is due to a breakdown in its bulk insulation caused by TEAM stress aging.

In some cases, discharges can be triggered on the surface of the insulation, which accelerates the aging of the insulation due to a interact between the surface charge accumulation and bulk charging [6]. Therefore, increasing the surface stability and aging resistance properties of EPR is very important for the safety operation of EPR. The electrical tracking and erosion resistance property was investigated using EPR by Du, and the discharge pattern of EPR, and the luminescence distribution and wavelet transform of discharge currents were calculated [7, 8]. Rajini investigated the tracking resistance of silicon rubber under AC and DC voltages, respectively. He found that the change in the variation of gamma dose affects the dielectric performance of silicon rubber under DC voltage, while no obvious change under AC voltage could be observed [9]. S.H. Kim studied the change of chemical bonds before and after tracking test of RTV silicon rubber using the ATR-FTIR method [10]. He found that the $SiCH_2OH$ or SiOH was generated during the process of electrical tracking discharge, which can be an indicator for aging of rubber. Loganathan studied the tracking and erosion resistance property of virgin and aged silicon rubber filled nano-sized SiO_2 under AC voltage. He found that the tracking and erosion resistance was improved when nano-filler concentration was increased in both the virgin and aged SIR composites [11].

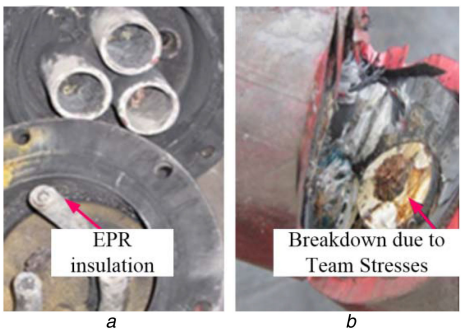

Fig. 1 *Aged EPR insulated cable withdrawn from a coal mine*
(a) Minging cable using EPR insulation, ***(b)*** Breakdown of EPR insulation

Surface modification can be a good way to change the surface property of materials without affecting their bulk property [12, 13]. Different material modification methods have been developed to tailor surface properties of dielectrics such as: suppressing the surface charge accumulation, increasing surface flashover voltage, and improving the surface anti-erosion property etc. [14]. In recent years, due to preferable results in a wide range of industrial applications, a direct fluorination technology has been applied to the dielectric materials [15, 16]. In this paper, EPR specimens were prepared and fluorinated for different duration. The morphology and element compositions of specimens were obtained. The surface potential decay (SPD) and complex permittivity were measured. The tracking discharge property at different stage were recorded, and the erosion properties after tracking test were studied. The potential mechanism of surface degradation of fluorinated

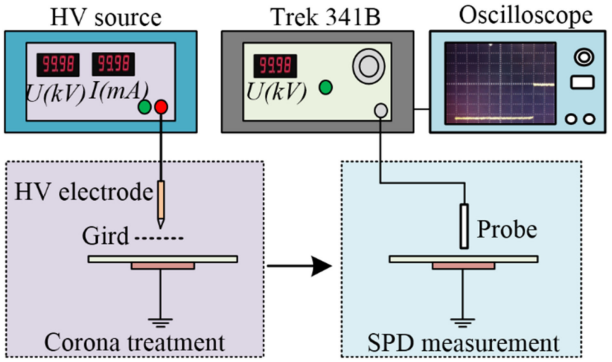

Fig. 2 *Schematic diagram of SPD measurement*

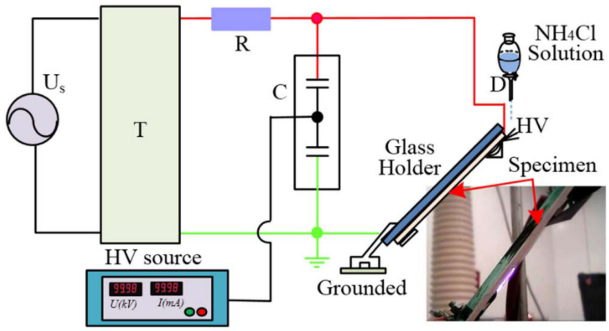

Fig. 3 *Schematic diagram of surface electrical tracking test for EPR*

specimens and the original specimen was discussed, and the recommended fluorination time duration for an optimised EPR surface property was proposed.

2 Specimen preparation and experimental setup

2.1 Specimen preparation

The specimen was prepared using EPR, DCJ30M. The raw material was preheated at 130°C for 1 min. After that, EPR was vulcanised at 165°C with a continuous pressure of 14 MPa for 15 min by a plate vulcanising device. The vulcanised EPR was heated and dried in a vacuum oven at 80°C for 24 h. The size of experimental specimen is $2 \times 140 \times 120$ mm^3.

The fluorination process was performed using an industrial fluorination device. Fluorination was carried out in a sealed stainless container and the F_2/N_2 volume ratio was 1:5. The reaction temperature was 50°C and the pressure was 0.1 MPa. The fluorination duration was 120, 240, 360 and 480 min, respectively.

2.2 Measurements of surface morphology and chemical properties

The surface morphology images of specimens were presented by a scanning electron microscope (TESCAN VEGA_3_SB). Surface chemical compositions of experiment specimens before and after fluorination were studied by energy dispersive spectroscopy (EDS; Oxford X-Max 20).

2.3 Measurements of electrical properties

The specimens were stored in a vacuum oven at 80°C for >24 h before the measurement [17–19]. Before SPD measurement, EPR specimens were placed between a grounded stainless-steel sheet to neutralise the surface charge of both surfaces.

The SPD measurement diagram is shown in Fig. 2. During the charging process, a needle-plate electrode was applied to generate charges on the surface of experimental specimens. A grid electrode was used to generate uniform surface charge distribution. The distance between the needle electrode tip and the specimen was 5 mm while the distance between the grid and the specimen was 2 mm. The grid area was 200 mm^2. The magnitude of needle and grid electrode was set to 6 and 2.4 kV, respectively. The charging time duration was 5 min. When the charging process was finished, experimental specimens were quickly placed under the probe for SPD detection [18].

The permittivity and the dielectric loss changes of experimental specimens at different frequency were measured by NOVOCONTROL Concept 80.

2.4 Surface tracking testing

The schematic diagram of electrical tracking measurement is shown in Fig. 3. The test device adheres to IEC 60587 standard [20]. The size of the specimen was $50 \times 120 \times 2$ mm^3. The AC voltage, Us, provided AC power voltage from 0 to 220 V. *T* is high voltage power transformer (YD-10kVA/100 kV). *R* was a resistor for protecting the transformer against over current. *C* was a voltage divider used to measure the voltage magnitude of the transformer. *V* was a voltmeter for monitoring the voltage amplitude of tracking discharge. *D* was a switch for controlling the drop speed of the NH_4Cl solution. During test, the specimen was set at a tilting plate which was with an angle of 45° to the horizontal plane. The filter papers were fixed between the HV electrode and the specimen, which could provide uniform droplet stream along the specimen surface. The contamination solution was prepared by 0.1% ammonium chloride (NH_4Cl). The flow rate of the droplet was controlled to 0.6 mL/min, which corresponded to the voltage amplitude of 4.0–4.75 kV. The test was stopped after 6 h, and then the specimens were taken out for characterising.

3 Experimental results

3.1 Surface morphology

The technique of surface fluorination is to use a mixer of fluorine gas and nitrogen to directly contact the surface of the specimen under a certain temperature and pressure. The surface chemical structure can thereby be modified, due to a strong oxidation of fluorine gas [21]. The surface fluorination is a process in which a hydrogen atom on the specimen surface being substituted to form a chain such as CH_2-CHF-CH_2–, –CHF-CH_2-CHF– and –CHF-CHF-CHF–.

Fig. 4 shows the surface morphology of EPR before and after fluorination. It can be found that the surface of the untreated specimen is flat and only very few scratch-like marks can be found which is probably due to the stress concentration during vulcanisation. After fluorination, it can be found on the surface that local roughness areas appear, and the roughness gradually increases with the fluorination time increasing from 120 to 240 min. The reason for this phenomenon may be due to the release of heat during the chemical chain replacement. The increase in the local temperature and non-uniform during fluorination result in uneven local stress on the specimen surface, and local protrusions. When the fluorination time is 360 min, a relatively flat surface could be found. This is because the fluorinated layer tends to be uniform over time, and local heat conduction can also promote the formation of the flat and compact surface layer. When the fluorination time is extended to 480 min, the flat surface layer becomes rough again with granular protrusions. This change is probably due to overheating and aging of the specimen after a long duration of fluorination.

Fig. 5 shows the surface morphology of experimental EPR after electrical tracking test. It can be observed that the surface is greatly damaged, especially for the untreated specimen and for the specimens fluorinated for 120 and 480 min. More holes and loose structures appear on the surface and large areas of layers can also be found in Figs. 5*a*, *b*, and *e*. While for specimens fluorinated for 240 and 360 min, the destroying degree after arc treatment is significantly reduced. Their surface compared with other specimens is more compact, and only small holes can be observed.

3.2 Element content

Fig. 6 shows the EDS of EPR fluorinated for different time duration. It can be found that oxygen (O) and carbon (C) absorption peaks appear in Fig. 6*a*, which are principle elements of

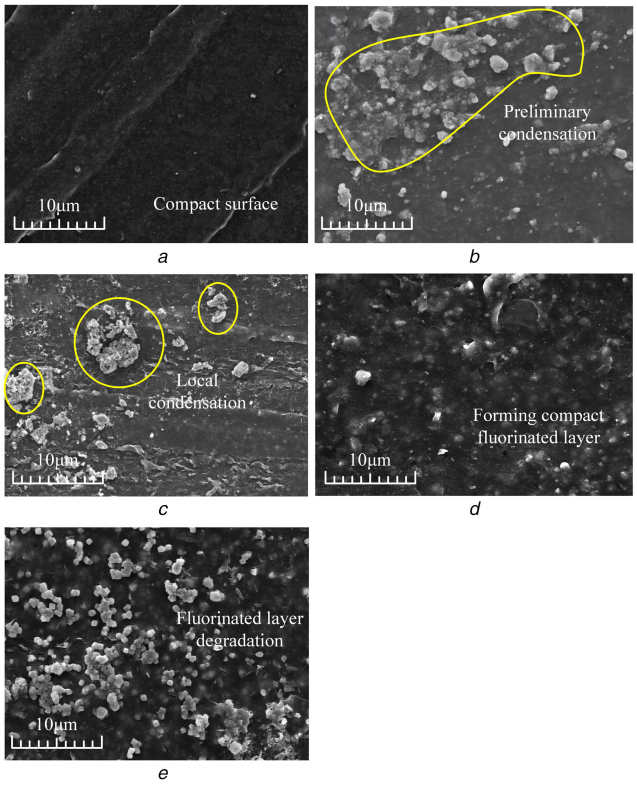

Fig. 4 *SEM images of EPR before and after fluorination*
(a) Original specimen, ***(b)*** F_120 min, ***(c)*** F_240 min, ***(d)*** F_360 min, and ***(e)*** F_480 min

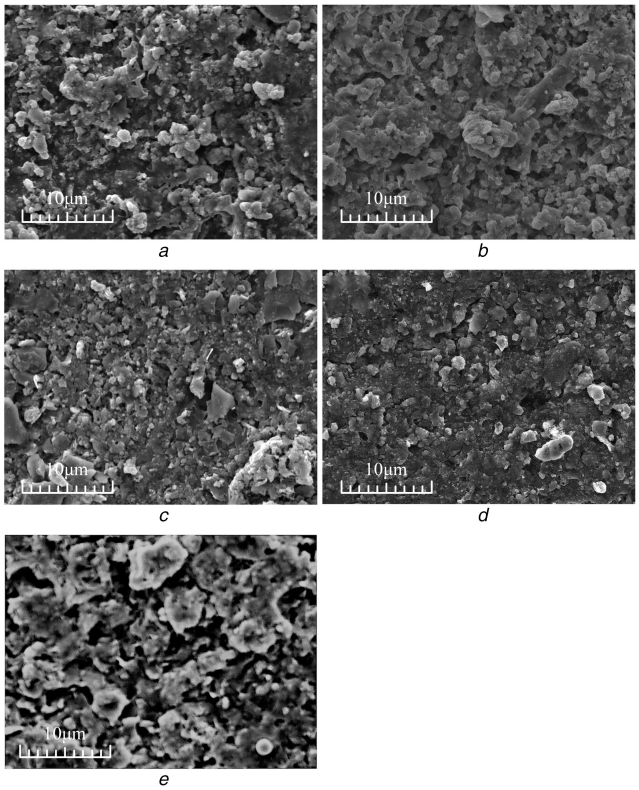

Fig. 5 *SEM images of experimental EPR after electric tracking test*
(a) Original specimen, ***(b)*** F_120 min, ***(c)*** F_240 min, ***(d)*** F_360 min, and ***(e)*** F_480 min

EPR. In Figs. 6*b–e*, the peak of fluorine element (F) is visible from spectrum due to the C–F bond formed after fluorination. As the fluorination reaction time increases, the fluorine content increases. To further confirm the changing law of different elements before and after fluorination, the variation of element mass percentage of

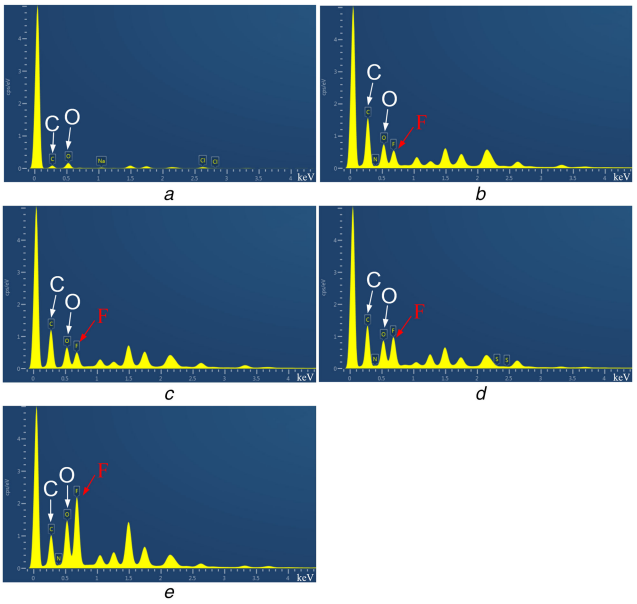

Fig. 6 *EDS spectrum of specimens with different fluorination time duration before electric tracking test*
(a) Original specimen, ***(b)*** Sample fluorinated for 120 min, ***(c)*** Sample fluorinated for 240 min, ***(d)*** Sample fluorinated for 360 min, and ***(e)*** Sample fluorinated for 480 min

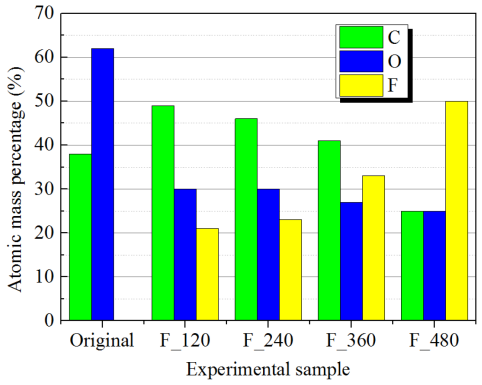

Fig. 7 *Element mass percentage of experimental specimens*

experimental specimens with different fluorination time duration is measured, as shown in Fig. 7. It can be found that the fluorine element is not included in the original specimen. The content of fluorine element increases with the fluorination time, while the carbon and oxygen contents decrease accordingly.

3.3 Surface potential decay

Fig. 8 shows the change of the normalised SPD with time. The decay rate, D, is described as the following formula [22]:

$$D = \frac{V(t_0) - V(t)}{V(t_0)} \times 100\% . \quad (1)$$

As can be seen from Fig. 8, the specimen fluorinated for 360 min and the untreated specimen have the slowest surface charge decay rate, while specimens fluorinated for 120, 240, and 480 min have a decay rate increasing with the increase of fluorination duration. The reasons for this phenomenon can be explained as follows: The fluorination reaction produces a C–F group on the surface, and the strong electronegativity of F atom can decrease the migration of charge carriers on the surface. In addition, F atoms on the surface can introduce a large number of deep traps and suppress the charge decay from the bulk. Thereby, it can be determined that the fluorination reaction can essentially suppress surface charge migration, which is why the charge dissipation rate for specimen fluorinated for 360 min is slightly slower than that of the untreated specimen. For specimens with fluorination times of 120, 240, and

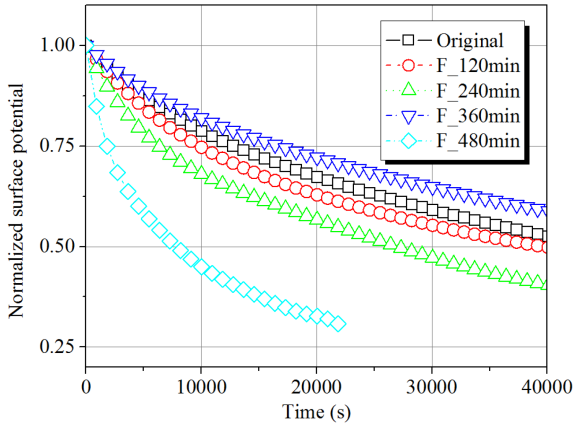

Fig. 8 *SPD curve of fluorinated specimens*

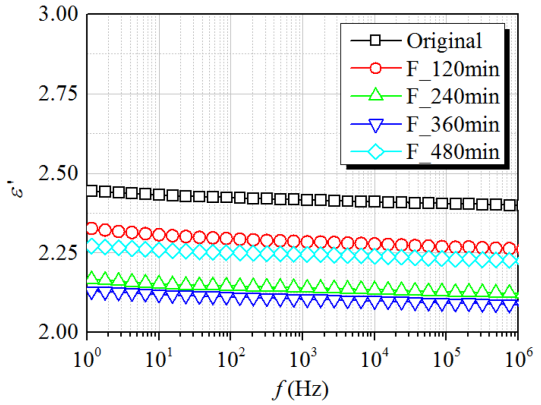

Fig. 9 *Real part of specimens, ε', at different frequency*

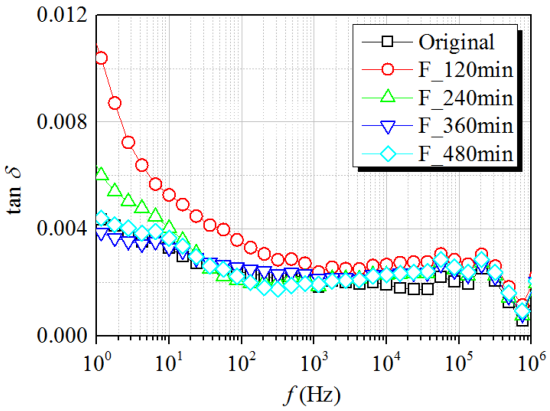

Fig. 10 *Dielectric loss factor of specimens, tanδ, at different frequency*

480 min, however, the fluorination reaction destroys the structure of the surface, making the surface tend to be rough. The increase in surface roughness can improve the surface hydrophilicity and promote the surface charge dissipation, which has already been verified in previous reports [23].

3.4 Dielectric properties and tracking

Fig. 9 shows the real part of experimental specimens, ε', at different frequency. The dielectric constant of the specimen before and after fluorination decreases with the increasing of frequency. As the fluorination duration gradually increases from 120 to 360 min, the real part of the dielectric constant gradually decreases from an initial value ~2.5 to ~2.1 in the test frequency range. This is mainly due to the introduction of a large number of C–F structures in the fluorinated layer. However, when the fluorination time is extended to 480 min, there is a rise in the real part of the dielectric constant, which is probably caused by the surface delamination due to excessive fluorination.

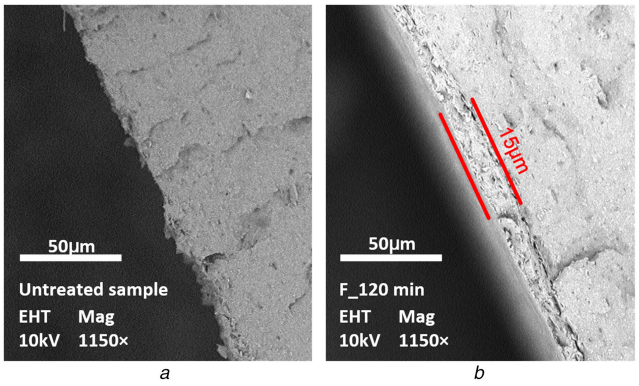

Fig. 11 *Cross-sectional view of an untreated specimen and the specimen fluorinated for 120 min*
(a) Untreated specimen, ***(b)*** Specimen fluorinated for 120 min

Fig. 10 shows the dielectric loss factor of specimens, tanδ, at different frequency. After fluorination, there is a certain fluctuation in the dielectric loss factor, especially in the low frequency after short-time fluorination. A slight increase trend can be found for specimens after fluoriantion. However, as the fluorination time is extended, the dielectric loss factor is gradually reduced, and the values tend to close to that of the untreated specimen. When the fluorination time is 360 min, the loss factor of the fluorinated specimen and the untreated specimen is substantially same within the measurement frequency range. While for the specimen fluorinated for 120 min, the increase of dielectric loss can be found, which is probably due to the water absorption caused by surface roughness.

Although, in Figs. 9 and 10, some trends about the dielectric properties of fluorinated and untreated specimens can be found, these trends do not have a particularly pronounced regularity, especially for short-time fluorinated specimens. The reason for the lack of regularity in dielectric properties may be due to local fluorination non-uniformity in short-time fluorination. The dielectric properties of specimen with uniformly fluorinated surfaces after long-term fluorination are basically the same compared with that of the untreated specimen. Fig. 11 is a cross-sectional view of an untreated specimen and the specimen fluorinated for 120 min. It can be seen that the thickness of the fluorinated layer is only 15 μm, which is <1% of the thickness of the specimen itself. Therefore, it can be believed that a stable fluorinated layer has little effect on the dielectric properties of the specimen matrix.

The process of discharge as well as images of specimens after tracking tests are shown in Figs. 12 and 13, respectively. The tracking discharge can be divided into two parts, including surface discharge and formation of carbon path. For initial discharge stage in Fig. 12*a*, the contamination fluid generates conduction current under the effect of high electric field. The micro spark appears at this stage due to the low discharge repetition rate and discontinuous discharge path. Fig. 12*b* shows the second stage of tracking discharge, at which the drying region is generated due to the heat concentration along surface of specimen and fluid evaporation. The spark discharge at this stage is brighter than that at the initial stage in Fig. 12*a*. Fig. 12*c* shows the stage of carbon path formation. During this stage, the continual sliding discharge and heat concentration make the molecular chain breakdown, and free carbon on the surface of the specimen forms the carbon path. Fig. 12*d* shows the breakdown stage of tracking. It can be seen that an arc discharge with intense light along the carbon path. At this stage, the high discharge frequency and heat accumulation make the surface breakdown occur quickly.

Fig. 14 shows the erosion weight, tracking length of specimens fluorinated for different time. The erosion weight is calculated by the weight deviations before and after tracking test. It can be found that the untreated specimen has a comparatively higher erosion weight of >0.32 g and the tracking length of >45 mm, which are more than that of the fluorinated specimens. For fluorinated specimens with different time duration, the change in erosion

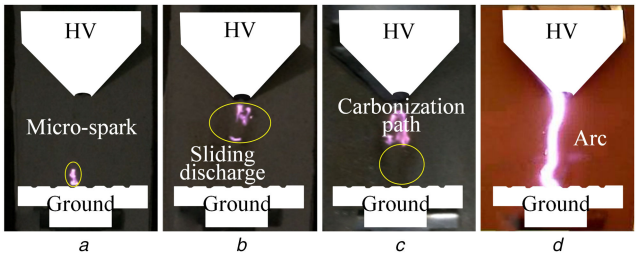

Fig. 12 *Tracking discharge process along EPR surface*
(a) Initial stage with micro spark on the surface, ***(b)*** Sliding discharge occurs on the surface, ***(c)*** Forming of carbonisation path due to discharge, ***(d)*** Breakdown and arc across the surface

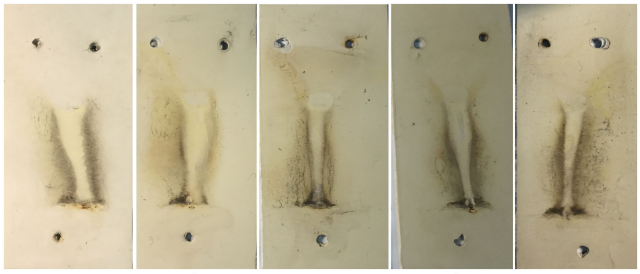

Fig. 13 *Images of specimens after tracking tests*
(a) Untreated, ***(b)*** F_120, ***(c)*** F_240, ***(d)*** F_360, ***(e)*** F_480

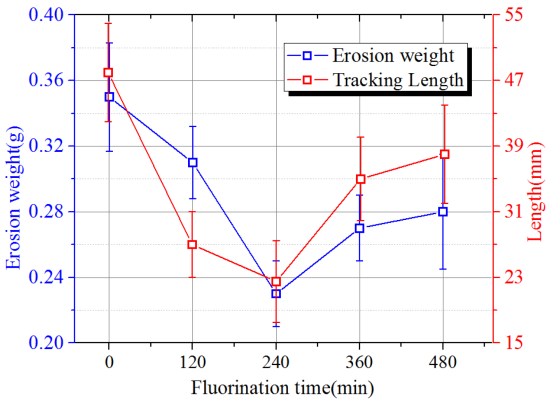

Fig. 14 *Relationship of the erosion weight and tracking length with the fluorinated time of EPR*

weight and length are not quite obvious. The change of the erosion weight ranges from 0.2 to 0.34 g, and the tracking length ranges from 16 to 42 mm.

4 Discussion

4.1 Surface charge transport

The charge transport mechanism schematic diagram of experimental specimens after tracking discharge is shown in Fig. 15. When the surface is fluorinated, the original C–H bond on the surface of the experiment specimen is replaced by a C–F structure, which makes the surface extremely electro-negative and chemically stable. Existing studies have shown that the introduction of C–F structures can introduce deeper carrier traps to the surface, thereby suppressing charge activity inside fluorinated coatings [21]. Therefore, the fluorinated surface can improve the surface stability and suppress the charge injection. Furthermore, the aging property of the surface under various electric fields can be improved. As a result, the aging resistance under arcing could be enhanced, as has already been discussed in Section 3.1 as well as our previous research [21]. Meanwhile, it can be seen from the EDS curve and the element content chart that the proportion of F element content is increased with the fluorination time increasing from 120 to 480 min. Even for specimens with the fluorinated time of 480 min, there is still no tendency of saturation for the mass

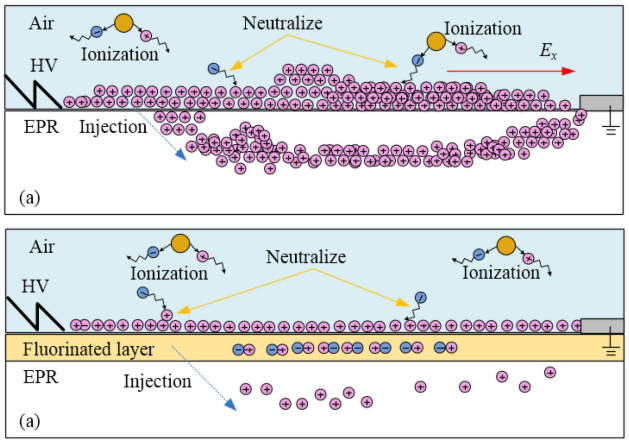

Fig. 15 *Charge transport mechanism diagram of experimental specimens after tracking discharge*

ratio of fluorine element, which indicates that the bond breaking process and the addition reaction of the fluorine atom is still in progress. This in turn verifies that the fluorination of EPR is a slow process compared with the fluorination results of epoxy [15]. It can also be noted that the original specimen has a lower carbon content than the oxygen content, which is most likely due to the surface-adsorbed oxygen-containing groups. The surface carbon content of specimens after fluorinated for 120 and 360 min is higher than the oxygen content, which is likely due to the fact that the fluorination process is an exothermic process, which causes the disappearance of surface oxygen-containing groups. After the specimen being fluorinated for 480 min, the surface shows obvious roughness and stratification. Such a surface is likely to promote the adsorption of water molecules in the air, which increases the surface oxygen content. It is also verified from the SEM image that the surface of specimen fluorinated after 480 min has a locally lamination structure which may be caused by the local surface expansion due to the local overheating under prolonged fluorination. This phenomenon can be an evidence accounting for that prolonged exposure to F_2 would have a negative effect on surface property of EPR.

In addition, the formation of a C–F structure on the surface after fluorination directly affects the transport properties of the charge on the surface under various electric field. Compared with the untreated specimen, the charge dissipation rate of specimen fluorinated for 360 min shows a decreasing trend, while those fluorinated for 120 and 240 min have an increasing trend. As it is already discussed in the former content, however, the fluorinated layer can introduce deep traps to restrain the charge injection from the surface to the bulk, which decreases the decay rate of surface charges. Moreover, the increase of surface roughness can be another factor influencing the surface conductivity, which directly affects charge decay rate [23]. The change in charge decay rate is the result of competition between surface morphology changing (to be more roughness) and chemical properties (introduction of C–H bonds). This is why the surface charge decay rate shows a first decrease and then increasing trend in Fig. 8.

4.2 Anti-aging property enhancement mechanism of fluorination

Being synthesised by ethylene, propylene and non-conjugated diene, EPR has excellent electro-chemical performance and corrosion resistant properties, which has been verified by our former research [18]. After corona treatment, the chemical reaction on the surface of EPR is hardly changed [18]. This is mainly due to the three-dimensional macro molecule network structure of EPR, formed by chemical reaction between the raw rubber and the vulcanising agent during the vulcanisation process. After being treated by fluorinate gas with suitable duration, the surface chemical property becomes more stable, due to the replacement of C–H structure by C–F structure.

The property of the electrical corrosion trace in Fig. 13 again verifies the correlation between the degree of fluorination and the arc aging resistance property of the specimen surface. When the fluorination time is 120 min, since the fluorinated layer has not yet been formed, the corrosion under the arc treatment is severe. When specimens are fluorinated for 120 to 360 min, the fluorinated layer gradually becomes stable, and the corrosion trace is relatively lowered. When the fluorination time is 480 min, the traces of corrosion shedding are significantly increased due to the instability of the sheet structure on the surface after prolonged fluorination. Surfaces with exfoliation and internal fluorination are relatively susceptible to arc aging.

Based on the above discussion, it can be obtained that there is an optimum fluorination time for the surface property of EPR. When the specimen is fluorinated for 360 min, the surface can form a dense fluorinated layer, and the phenomenon of local condensation cannot be observed on the surface any more. Combined with the surface condition after arc aging, it is further concluded that the surface structure damage of the specimen under 360 min fluoridation duration decreased significantly, while the untreated specimen and the fluorinated specimen with 120, 240, and 480 min showed a more serious aging layered structure. Although an increasing of surface charge decay rate can be found for specimens fluorinated for 120 and 240 min, an increasing of surface charge decay rate could be useful for a decreasing of local electric field distortion. However, it is still believed that fluorination for 360 min is the recommended fluorination option. The reason is as follows: SEM image shows that the fluorinated layer is not particularly stable after a short period of fluorination, which is manifested by an increase in surface roughness. The change in the rate of charge dissipation for short time fluorinated specimens is due to an increase in surface roughness, while the rate of charge dissipation does not increase much compared with that of untreated specimens.

5 Conclusion

In this work, the effect of various fluorinated duration on the surface electrical tracking properties of EPR was studied. Detailed conclusions are shown as follows:

1. The surface morphology of EPR can be modified by controlling fluorination duration. When the fluorination duration was 120 and 360 min, the surface morphology gradually becomes flat and compact as the fluorination time is prolonged. However, a fluorination duration of 480 min can results in a rough surface condition, which results in a reduction in the resistance to electrical tracking.
2. The fluorinated layer can introduce deep traps to restrain the charge injection from the surface to the bulk. This would decrease the decay rate of surface charges. However, the increase of surface roughness can be another factor influencing the surface conductivity, which directly affects charge decay rate. The change in charge decay rate is the result of competition between surface morphology changing (to be more roughness) and chemical properties (introduction of C–H bonds).
3. The recommended fluorination time duration for an optimised surface property is ∼360 min for EPR specimen.

6 Acknowledgment

This study is financially supported by National Natural Science Foundation of China (51577123, 51807060 and 51737005).

7 References

[1] Du, B.X., Li, Z.L., Li, J.: 'Surface charge accumulation and decay of direct-fluorinated RTV silicone rubber. *IEEE Trans. Dielectr. Electr. Insul.*, 2014, **21**, (5), pp. 2338–2342

[2] Han, T., Du, B.X., Su, J.G.: 'Electrical tree initiation and growth in silicone rubber under combined DC-pulse voltage', *Energies*, 2018, **11**, (4), p. 764

[3] Lei, Z, Song, J, Tian, M, *et al.*: 'Partial discharges of cavities in ethylene propylene rubber insulation', *IEEE Trans. Dielectr. Electr. Insul.*, 2014, **21**, pp. 1647–1659

[4] Zuidema, C., Kegerise, W., Fleming, R., *et al.*: 'A short history of rubber cables', *IEEE Electr. Insul. Mag.*, 2011, **27**, (4), pp. 45–50

[5] Li, C., Lin, C., Hu, J., *et al.*: 'Novel HVDC spacers by adaptively controlling surface charges - part I: charge transport and control strategy', *IEEE Trans. Dielectr. Electr. Insul.*, 2018, **25**, pp. 1238–1247

[6] Lei, Z., Li, C., Men, R., *et al.*: 'Mechanism of bulk charging behavior of ethylene propylene rubber subjected to surface charge accumulation', *J. Appl. Phys.*, 2018, **124**, p. 244103

[7] Du, B.X., Li, Z.L., Li, J.: 'Effects of direct fluorination on space charge accumulation in HTV silicone rubber', *IEEE Trans. Dielectr. Electr. Insul.*, 2016, **23**, (4), pp. 2353–2360

[8] Du, B.X., Liu, Y.: 'Pattern analysis of discharge characteristics for hydrophobicity evaluation of polymer insulator', *IEEE Trans. Dielectr. Electr. Insul.*, 2011, **18**, (1), pp. 114–121

[9] Rajini, V., Udayakumar, K.: 'Degradation of silicone rubber under AC or DC voltages in radiation environment', *IEEE Trans. Dielectr. Electr. Insul.*, 2009, **16**, pp. 834–841

[10] Kim, S.-H., Cherney, E.A., Hackam, R., *et al.*: 'Chemical changes at the surface of RTV silicone rubber coatings on insulators during dry-band arcing', *IEEE Trans. Dielectr. Electr. Insul.*, 1994, **1**, (1), pp. 106–123

[11] Mohamad, A., Chen, G., Zhang, Y., *et al.*: 'Moisture effect on surface fluorinated epoxy resin for high-voltage DC applications', *IEEE Trans. Dielectr. Electr. Insul.*, 2016, **23**, (2), pp. 1148–1155

[12] Shao, T., Yang, W.J., Zhang, C., *et al.*: 'Enhanced surface flashover strength in vacuum of polymethylmethacrylate by surface modification using atmospheric-pressure dielectric barrier discharge', *Appl. Phys. Lett.*, 2014, **105**, p. 071607

[13] Yu, K.K., Zhang, G.J., Zheng, N., *et al.*: 'Effect of laser treatment on the surface flashover characteristics of alumina ceramic in vacuum', *Discharges Electr. Insul. Vacuum*, 2008, **2**, pp. 495–498

[14] Xie, Q., Liang, S., Fu, K., *et al.*: 'Distribution of polymer surface charge under DC voltage and its influence on surface flashover characteristics', *IEEE Trans. Dielectr. Electr. Insul.*, 2018, **25**, (6), pp. 2157–2168

[15] Li, C.Y., He J, L., Hu, J.: 'Surface morphology and electrical characteristics of direct fluorinated epoxy-resin/alumina composite', *IEEE Trans. Dielectr. Electr. Insul.*, 2016, **23**, pp. 3071–3077

[16] Du, B.X., Li, Z.L.: 'Hydrophobicity, surface charge and dc flashover characteristics of direct-fluorinated RTV silicone rubber', *IEEE Trans. Dielectr. Electr. Insul.*, 2015, **22**, (2), pp. 934–940

[17] Simmons, J.G., Tam, M.C.: 'Theory of isothermal currents and the direct determination of trap parameters in semiconductors and insulators containing arbitrary trap distributions', *Phys. Rev. B*, 1973, **7**, pp. 3706–3716

[18] Li, C., Lin, C., Zhang, B., *et al.*: 'Understanding surface charge accumulation and surface flashover on spacers in compressed gas insulation', *IEEE Trans. Dielectr. Electr. Insul.*, 2018, **25**, (4), pp. 1152–1166

[19] Zhang, J.W., Cao, D.K., Cui, Y.C., *et al.*: 'Influence of potential induced degradation phenomena on electrical insulating backsheet in photovoltaic modules', *J. Clean Prod.*, 2018, **208**, pp. 333–339

[20] IEC publication 60587: 'Testing method for evaluating the resistance of tracking and erosion of electrical insulating materials used under severe ambient conditions', 1984

[21] Li, C., Hu, J., Lin, C., *et al.*: 'Fluorine gas treatment improves surface degradation inhibiting property of alumina-filled epoxy composite. *AIP. Adv.*, 2016, **6**, (2), p. 025017

[22] Chen, G.: 'A new model for surface potential decay of corona-charged polymers', *J. Phys. D, Appl. Phys.*, 2010, **43**, pp. 55405–55411(7)

[23] Xue, J., Wang, H., Chen, J., *et al.*: 'Effects of surface roughness on surface charge accumulation characteristics and surface flashover performance of alumina-filled epoxy resin spacers', *J. Appl. Phys.*, 2018, **124**, (8), p. 083302